Winter October 27, 2012

Speed sensorless torque control of an IPMSM drive with online stator resistance estimation using reduced order EKF

Emad Gameil Shehata, E. G. Shehata

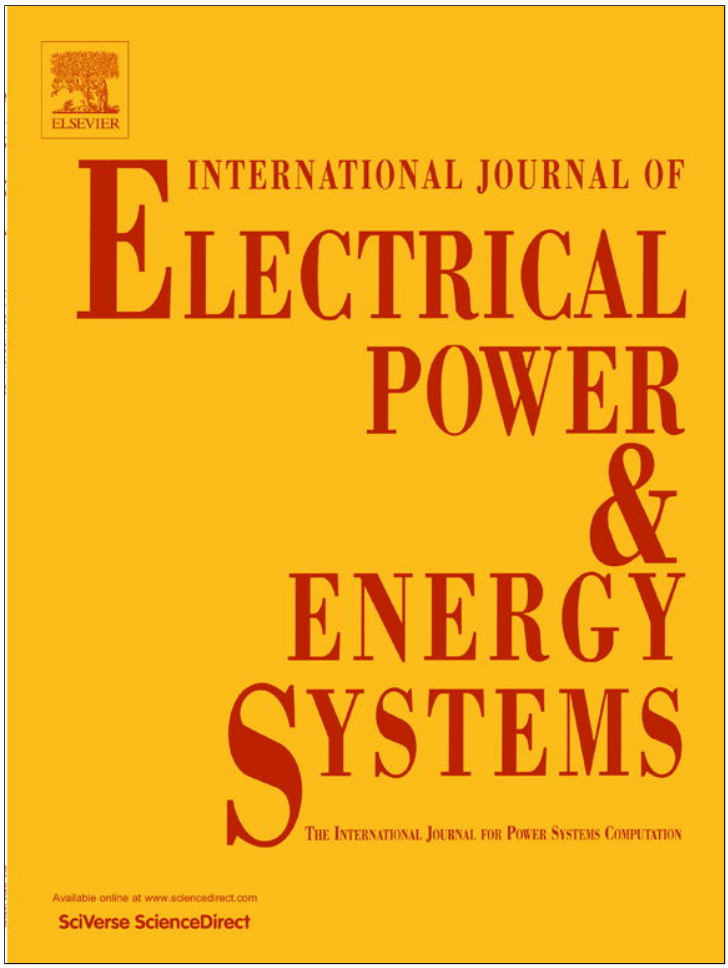

(This is a sample cover image for this issue. The actual cover is not yet available at this time.)

Electrical Power and Energy Systems 47 (2013) 378–386

Contents lists available at SciVerse ScienceDirect

Electrical Power and Energy Systems

journal homepage: www.elsevier.com/locate/ijepes

Speed sensorless torque control of an IPMSM drive with online stator resistance estimation using reduced order EKF

E.G. Shehata *

Electrical Engineering Dept., Faculty of Engineering, Minia University, Egypt

ARTICLE INFO

Article history:
Received 27 August 2011
Received in revised form 22 July 2012
Accepted 27 October 2012

Keywords:
Active flux concept
Speed sensorless torque control
Sliding mode controller
Reduced order EKF

ABSTRACT

Speed sensorless control of an interior permanent magnet synchronous motor (IPMSM) based on direct torque control (DTC) is proposed in this paper. The rotor speed and position of the IPMSM are estimated based on an active flux concept, where, the active flux vector position is identical to the rotor position. The proposed algorithm does not require neither high frequency injection signal nor complicated schemes even at vary low speed operation. Torque/ flux sliding mode controller (SMC) combined with space vector modulation is proposed to improve the performance of the classical DTC. Stator resistance value is required for a stator flux and electromagnetic torque estimation. Its variation due to temperature or frequency degrades the scheme performance, especially, at low speed operation. To overcome this problem, a reduced order extended Kalman filter (EKF) is proposed to update online the stator resistance. The advantages of the direct torque control, sliding mode controller, and speed sensorless control are incorporated in the proposed scheme. Simulation works are carried out to show the ability of the proposed scheme at different operating conditions. The results demonstrate the activity of the scheme at wide range speed operation with load disturbance and parameters variation.

1. Introduction

Permanent magnet synchronous motors have received a greet attention in the recent years for drive application. The interior permanent magnet synchronous motor has several advantages such as a high efficiency due to the reluctance torque and high power density. Speed control of the IPMSM needs the acknowledgment of the rotor speed; however, the speed sensors have several drawbacks such as reliability, machine size and drive cost [1–3]. Different algorithms are studied for speed sensorless of the IPMSM [1–8]. The popular algorithm utilizes the extended emf estimation in a rotating reference frame [1–3]. This type gives a good performance at medium and high speed operation; however, it fills at low speed and standstill operation because the back emf is proportional to the motor speed. A start-up algorithm is required when the motor at a standstill or at a low speed operation. In addition, the measured voltage and current are transformed into a new rotating frame. Another algorithm utilizes the stator inductance variation based on the relative position of the rotor [4–6]. In Ref. [4], a high frequency voltage signal/pulse is injected in the stator winding. The rotor position is extracted from the measured current signal response. In Ref. [5], the inductance matrix including the rotor position information is determined from current harmonics produced by the switching operations of an inverter driving the IPMSM. Speed information can be obtained from the position information. This algorithm gives a good performance at low speed and standstill operation, however, the generation of the high frequency signal increases the drive complicity and the motor losses. In addition, a negative torque can be generated and degrades the scheme performance. In [7], the extended emf estimation and the signal injection algorithms are used together for position sensorless control. At standstill, the rotor position is estimated by a signal injection algorithm. After the starting period, the extended emf estimation algorithm is applied.

The observers or the estimators have been widely used for system state estimation [8–11]. In Ref. [8], a linear model of the IPMSM on the stationary reference frame is constructed and a position observer is designed based on γ-positive real problem. However, large error in the speed appears at rated speed operation. Moreover, the sensorless control at low speed with load torque cannot realized successfully. In Ref. [9], the rotor position is estimated without any voltage measurement, where, an unknown input observer estimates the applied voltage to the motor from the measured current. Full order extended Kalman filter is designed for flux and speed/position estimation of IPMSM [10,11]. However, the computational burden is the main drawback of the full order EKF.

A Sliding mode observer is used for speed sensorless control [12–15]. The sliding mode observer has robustness against parameters variation; however, the chattering phenomenon is considered

* Tel.: +20 1271216894.
E-mail address: emadgameil@eng.miniauniv.edu.eg

0142-0615/$ - see front matter © 2012 Elsevier Ltd. All rights reserved.
http://dx.doi.org/10.1016/j.ijepes.2012.10.068

Nomenclature

v_{abc}	three phase stator voltages	i_{abc}	three phase stator currents
S_{abc}	switching state of the inverter	v_α, v_β	stationary axes voltage components
i_α, i_β	stator current components in stationary frame	V_d^*, V_q^*	reference voltage in synchronous frame
ϕ_d, ϕ_q	stator flux components in synchronous frame	$\hat{\phi}_\alpha$, $\hat{\phi}_\beta$	estimated stator flux components
ϕ_s^*	the reference stator flux vector amplitude	$\hat{\phi}_s$	estimated stator flux amplitude
ϕ_f	permanent magnet flux	ω_r, $\hat{\omega}_r$	actual, estimated rotor speed
ω_r^*	reference rotor speed	$\hat{\theta}_e$	estimated angular rotor position
$\hat{\theta}_s$	estimated stator flux position	γ	voltage vector angle with respect to *d*-axis
T_e	electromagnetic torque	L_d, L_q	stator inductances
R_s, $\widehat{R}_s$	actual and estimated stator resistance	P	number of pole pairs

its main drawback. In Refs. [16,17] the sliding mode observer is proposed for emf estimation, then, EKF is used for speed estimation based on the estimated emf. In Refs. [18,19] a variable structure observer is used for stator flux estimation. This observer used a combined voltage–current model at low speed and switched to a voltage model at high speed. High frequency voltage rotating injection scheme is used to obtain the rotor position which required for current model at low speed operation. In addition, the rotor speed is estimated from the estimated stator flux speed with a dynamic correction algorithm.

In Ref. [20], the rotor position is estimated from subtract of the stator flux position and the load torque angle, however, speed errors appear especially at low speed operation with load disturbance. In Refs. [21,22], active flux concept is proposed for rotor position and speed estimation of the IPMSM. Wide speed sensorless control is obtained without any signal injection. Moreover, the estimation algorithm is very simple compared to the others. In spite of the advantages of the active flux observer, a stator resistance variation due to temperature and/or frequency effects badly on the estimation accuracy and the control system may fill at low speed operation [23].

To overcome the effect of stator resistance variation, different algorithms are designed for stator resistance estimation online [23–25]. In Ref. [23], a proportional–integral (PI) controller is designed for online stator resistance compensation based on the flux error between the reference and estimated values. In Ref. [24], a Lyapunov algorithm is used to estimate the rotor speed and the stator resistance, however, the variation of stator resistance at different speed and load operation had not been studied. In Ref. [25], the stator resistance and the back emf coefficient of PMSM are estimated online. The algorithm is based on a steady state equations and linearly perturbed equations of the PMSM dynamics about the operating point. A sinusoidal current component is superimposed in the direct axis current command when the speed command reaches the steady state.

In this paper, the speed sensorless control of the IPMSM based direct torque control is proposed. To overcome the drawbacks of the classical DTC, a torque/ flux SMC combined with space vector modulation is designed to improve its performance. In the proposed scheme, the SMC replaces the hysteresis comparators and lookup table of the classical DTC. For speed sensorless control based on DTC, active flux concept is proposed for speed and position online estimation. Active flux vector is estimated from the measured voltage and current signals. The proposed scheme does not require neither additional complicated algorithms nor signal injection schemes. Finally, to overcome the stator resistance variation problem, a reduced order EKF is designed to update the stator resistance value online. The model uncertainties and nonlinearities are well suited to the stochastic nature of EKF. Finally, computer works are carried out to evaluate the proposed scheme during low and high speed operation with parameters variation.

2. Direct torque control of IPMSM drive

Direct torque control is considered the simplest torque controller for industrial applications. For IPMSM, the torque equation can be expressed as a function of the load angle (δ) as [26,27]:

$$T_e = \frac{3P|\phi_s|}{4L_dL_q}[2\phi_f L_q \sin\delta - |\phi_s|(L_q - L_d)\sin 2\delta] \quad (1)$$

It is shown that the motor torque depends on the amplitude of the stator flux and the load angle. With constant stator flux amplitude, the torque can be controlled depend on the load angle. The load angle can be controlled by controlling the stator flux speed with respect to the rotor flux.

The stator flux vector is estimated from the integration of the stator back emf as follows:

$$\hat{\phi}_\alpha = \int (v_\alpha - R_s i_\alpha)dt + \phi_\alpha(0) \quad (2)$$

$$\hat{\phi}_\beta = \int (v_\beta - R_s i_\beta)dt + \phi_\beta(0) \quad (3)$$

where $\phi_\alpha(0)$ and $\phi_\beta(0)$ are the initial values of the stator flux components.

The pure integrator can be modified by implementing it applying a low-pass filter (LPF). However, LPF will produce errors in magnitude and phase angle especially if the excitation frequency is lower than the cutoff frequency of the LPF. Several improved estimation methods have been investigated [28].

The stator flux amplitude and position are estimated as follows:

$$\hat{\phi}_s = \sqrt{\hat{\phi}_\alpha^2 + \hat{\phi}_\beta^2} \quad (4)$$

$$\hat{\theta}_s = a\tan\left(\frac{\hat{\phi}_\beta}{\hat{\phi}_\alpha}\right) \quad (5)$$

The electromagnetic torque can be estimated from the measured current and estimated stator flux as:

$$\widehat{T}_e = 1.5P(i_\beta\hat{\phi}_\alpha - i_\alpha\hat{\phi}_\beta) \quad (6)$$

The previous equations show that the stator resistance is the only required parameter.

For classical DTC, the torque, flux errors and the flux position angle are fed to a switching table which selects the switching states of the inverter. The classical DTC has disadvantages such as high torque and stator flux ripples and variable switching frequency [29,30]. In addition, stator resistance variation degrades the DTC performance, especially, at low speed operation. Several

techniques are proposed to reduce the ripples and fix the switching frequency, i.e., [31,32].

3. Torque/flux SMC for an IPMSM drive

Sliding mode controller has been proposed to improve the performance of classical DTC. Sliding mode control technique is an effective, high frequency switching control strategy for nonlinear systems with uncertainities. It can offer many good properties such as good performance against unmodeled dynamics, insensitivity to parameters variation, external disturbance rejection and fast dynamic response [33–35]. DTC can be considered to be a special case of the sliding mode controller [36].

The problem of sliding mode controller design is the determination of a suitable switching surface that yields desired dynamic properties, and a suitable control input (using state feedback) that forces the instantaneous state to move along the chosen surface [33,34]. The SMC is designed to generate the stator voltage reference components from the torque and flux errors. Two integral switching functions are used for torque and flux control. The stator voltage command is generated based on the two integral switching functions. Space vector modulation is combined with the SMC to provide constant switching frequency and high voltage resolution.

The switching functions of the torque and flux are chosen as:

$$s_T = K_p e_T + K_i \int_0^t e_T dt \tag{7}$$

$$s_\phi = K_p e_\phi + K_i \int_0^t e_\phi dt \tag{8}$$

where

$$e_T = T_e^* - \hat{T}_e \tag{9}$$

$$e_\phi = \phi_s^* - \hat{\phi}_s \tag{10}$$

and K_p, K_i are positive gains.

The stator flux linkage amplitude and the electromagnetic torque can be estimated respectively in the synchronous reference frame as follows:

$$\hat{\phi}_s = \left(\phi_d^2 + \phi_q^2\right)^{0.5} \tag{11}$$

$$\hat{T}_e = 1.5P(\phi_d i_q - \phi_q i_d) \tag{12}$$

The task is to design a control law that drive the state trajectory to the intersection of the surfaces described earlier. The time differentiation of the sliding surfaces can be expressed as follows:

$$\dot{s}_T = K_p \dot{e}_T + K_i e_T \tag{13}$$

$$\dot{s}_\phi = K_p \dot{e}_\phi + K_i e_\phi \tag{14}$$

Using Eqs. (1–3) and (9–12), the previous two Eqs. (13) and (14) will yield:

$$\dot{s} = M + F - Du \tag{15}$$

where

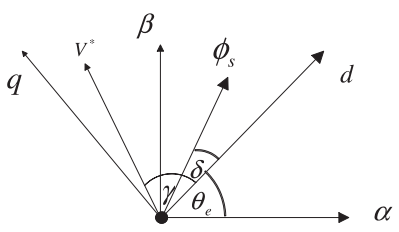

Fig. 1. Space position of the stator voltage and flux vectors.

$$\dot{s} = \begin{bmatrix} \dot{s}_T \\ \dot{s}_\phi \end{bmatrix}, \quad M = \begin{bmatrix} K_i e_T + K_p \dot{T}_e^* \\ K_i e_\phi + K_p \dot{\phi}_s^* \end{bmatrix}, \quad F = \begin{bmatrix} -1.5PK_p(L\phi_q)f_1 + \left(L\phi_d + \frac{\phi_f}{L_d}\right)f_2 \\ -\frac{K_p}{\phi_s}(\phi_d f_1 + \phi_q f_2) \end{bmatrix},$$

$$f(x) = \begin{bmatrix} f_1 \\ f_2 \end{bmatrix} = \begin{bmatrix} -\frac{R_s}{L_q}\phi_q - \omega_e \phi_d \\ -\frac{R_s}{L_d}(\phi_d - \phi_f) + \omega_e \phi_q \end{bmatrix},$$

$$D = \begin{bmatrix} 1.5PK_p\left(L\phi_d + \frac{\phi_f}{L_q}\right) & 1.5PK_p L\phi_q \\ \frac{K_p}{\phi_s}\phi_q & \frac{K_p}{\phi_s}\phi_d \end{bmatrix},$$

$$u = [V_q \quad V_d]^T \text{ and } L = \frac{1}{L_q} - \frac{1}{L_d}$$

Taking the uncertainties into account, Eq. (15) will become

$$\dot{s} = M + F_n - D_n u + W \tag{16}$$

where D_n and F_n are the nominal values of D and F, respectively and W is the lumped uncertainty which can be expressed as

$$W = \begin{bmatrix} W_T \\ W_\phi \end{bmatrix} = \Delta F + \Delta D u \tag{17}$$

Putting $\dot{s} = 0$, the control effort law (reference voltage u^*) can be deduced as

$$u^* = D_n^{-1}(M + F_n + \alpha sign(s)) \tag{18}$$

where

$$u^* = \left[V_q^* \quad V_d^*\right]^T, \quad \alpha \geqslant |W|, \quad \alpha = \begin{pmatrix} \alpha_T \\ \alpha_\phi \end{pmatrix},$$

and α_T, α_ϕ are positive gains.

The stator flux and the torque can be regulated by the stator voltage components. The highly nonlinear and coupled dynamics of the matrices $\left(D_n^{-1}, F_n\right)$ complicate the design of the SMC. However, if the stator flux amplitude is controlled to be constant, the variables of the matrices $\left(D_n^{-1}, F_n\right)$ can be analyzed as bounded disturbances regulating the stator flux and the torque. So, it can be added to the lumped uncertainties. The control effort equation can be expressed as:

$$u^* = M_1 + \alpha_1 sign\ (s) \tag{19}$$

where $M_1 = D_n^{-1} M$ and $\alpha_1 = \left|D_n^{-1}(F_n + \alpha)\right|$

The control effort is designed in Eq. (19) such that the system trajectory is forced towards the sliding surface. However, this control strategy produces some drawbacks associated with large control chattering that may wear coupled mechanisms and excite unstable system dynamics. In addition, the sensitivity of the controlled system to uncertainties still exists in the reaching phase. To reduce the chattering in the control effort, The function $sat(s)$ is used instead of $sign(s)$. In addition, a total sliding mode control idea is chosen, to overcome the reaching phase problem. The control effort of the total torque/flux SMC can be written as:

$$u^* = M_1 + \alpha_1\ sat(s) + K_c s + \begin{bmatrix} K_T \hat{T}_e \\ K_\phi \hat{\phi}_s \end{bmatrix} \tag{20}$$

where $sat(s) = \frac{s}{|\lambda|+s}$, and K_T, K_ϕ,K_c and λ are positive gains.

The third and fourth terms are added in Eq. (20) to insure the stability of the SMC during reaching phase. The stability of the proposed SMC is proved using Lyapunov stability theorem in the Appendix A.

The reference voltage amplitude and position are estimated as follows:

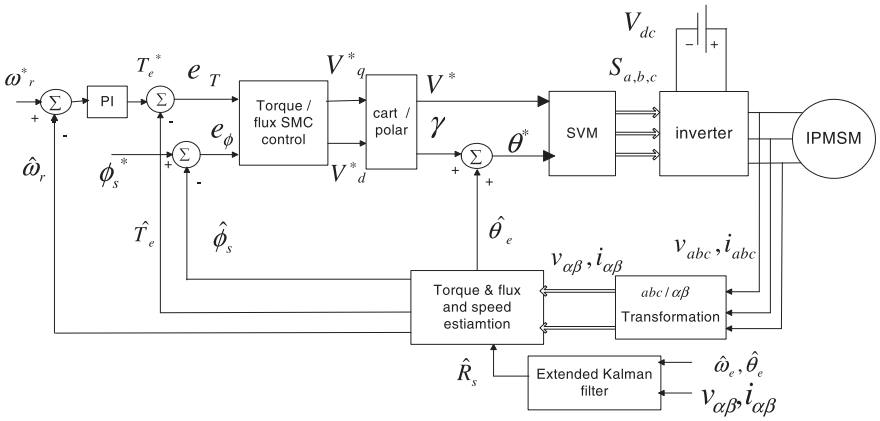

Fig. 2. Block diagram of the sensorless torque/flux SMC-SVM scheme.

$$V^* = \sqrt{V_d^{*2} + V_q^{*2}} \tag{21}$$

$$\gamma = \tan^{-1}\left(\frac{V_q^*}{V_d^*}\right) \tag{22}$$

As shown in Fig. 1, the reference voltage position with respect to α-axis in a stationary frame is expressed as:

$$\theta^* = \gamma + \hat{\theta}_e \tag{23}$$

where $\hat{\theta}_e$ is the estimated active flux (rotor) position angle.

The block diagram of the torque/flux SMC of the IPMSM is shown in Fig. 2. The stator flux and electromagnetic torque are estimated from the measured voltage and current signals. The rotor position and speed are estimated from the stator flux and current based on the active flux concept as will be explained in the following section. The measured voltage, current signals, the estimated rotor speed and position are fed to the reduced order EKF to estimate online the stator resistance which used to update estimation of the stator and active fluxes. The estimated and reference speed values are compared and the error is fed to a PI controller to generate the reference torque. The reference and estimated values of the torque and stator flux are compared and the errors are fed to the torque/ flux SMC to estimate the reference stator voltage in the synchronous frame which fed to the space vector modulation to determine the inverter state.

4. Speed and position estimation

The concept of active flux for the IPMSM is defined as follows [22]:

$$\phi^a = \phi_f + (L_d - L_q) i_d \tag{24}$$

It can be noticed that the active flux vector is aligned the d-axis of the rotor frame.

The stator flux component in the synchronous reference frame is expressed as follows:

$$\begin{bmatrix} \phi_d \\ \phi_q \end{bmatrix} = \begin{bmatrix} L_d & 0 \\ 0 & L_q \end{bmatrix} \begin{bmatrix} i_d \\ i_q \end{bmatrix} + \begin{bmatrix} \phi_f \\ 0 \end{bmatrix} \tag{25}$$

Using Eqs. (25) and (24) can be rewritten as:

$$\phi^a = \phi_d - L_q \, i_d \tag{26}$$

Second equation of (25) can be expressed as:

$$0 = \phi_q - L_q \, i_q \tag{27}$$

Combining Eqs. (26) and (27), the active flux can be described in the space phasor form as:

$$\bar{\phi}^a = \bar{\phi}_s - L_q \, \bar{i}_s \tag{28}$$

where $\bar{\phi}^a$, $\bar{\phi}_s$ and $\bar{i}_s$ are the active flux, stator flux and stator current space vectors, respectively.

The previous equation can be expressed as:

$$\bar{\phi}^a = \int (\bar{V}_s - R_s \bar{i}_s) dt - L_q \bar{i}_s \tag{29}$$

Eq. (29) indicates that the active flux vector can be estimated using the measured stator voltage and current signals.

The active flux or rotor position angle is estimated as:

$$\hat{\theta}_e = \tan^{-1}\left(\frac{\hat{\phi}_\beta^a}{\hat{\phi}_\alpha^a}\right) \tag{30}$$

where $\hat{\phi}_\alpha^a$ and $\hat{\phi}_\beta^a$ are the stationary components of the active flux vector.

The rotor speed can be estimated from the time differentiation of Eq. (30) as:

$$\hat{\omega}_r = \frac{1}{P}\frac{d\hat{\theta}_e}{dt} = \frac{1}{P}\frac{\left(\hat{\phi}_\alpha^a\right)_{k-1} \cdot \left(\hat{\phi}_\beta^a\right)_k - \left(\hat{\phi}_\beta^a\right)_{k-1} \cdot \left(\hat{\phi}_\alpha^a\right)_k}{T_s \cdot \left[\left(\hat{\phi}_\alpha^a\right)_k^2 + \left(\hat{\phi}_\beta^a\right)_k^2\right]} \tag{31}$$

where the active flux components are calculated at the samples k and $k-1$, and T_s is the sampling interval.

5. Stator resistance estimation

As shown in the previous sections, the stator flux estimation and in turn the active flux estimation depends mainly on the stator resistance. The stator resistance changes as a result of the temperature or frequency. At high speeds, the stator resistance voltage drop is small compared to the stator voltage. At low speeds, this drop becomes the dominant. Therefore, any change in stator resistance gives wrong estimation of the stator flux and consequently the electromagnetic torque and the stator flux position. An error in the stator flux position is more important as it can cause the controller to select a wrong switching state which can result in failure of the controller. Moreover, in the case of sensorless speed control, the mismatched stator resistance introduces an error in the position and speed estimation. Online estimation of stator resistance can improved the performance at wide range of speed operation. In this paper, a reduced order EKF is proposed to estimate the stator resistance. The model uncertainties and nonlinearities are well suited to the stochastic nature of EKF. This is the reason why the EKF has found wide application in sensorless control. In

Table 1
Parameters and data of the IPMSM [35].

No. of pole pairs	2	Base speed ω (rpm)	1500
Rs (Ω)	6	Magnet flux linkage Φ_f (Wb)	0.337
Lq (H)	0.1024	Rated torque Te (N m)	3
Ld (H)	0.0448	Vdc (volt)	300

addition, the proposed reduced order EKF does not suffer from the computational burden problem of the full order type.

The IPMSM dynamic model can be expressed in the stationary reference frame as:

$$[\dot{x}] = [A][x] + [B][u] \tag{32}$$

$$[y] = [C][x] \tag{33}$$

$$\text{where} \quad [x] = [\, i_\alpha \quad i_\beta \quad R_s \,]^T \tag{34}$$

$$[u] = [\, v_\alpha \quad v_\beta \quad \hat{\omega}_e \,] \tag{35}$$

$$[C] = \begin{bmatrix} 1 & 0 & 0 \\ 0 & 1 & 0 \end{bmatrix} \tag{36}$$

The matrix parameters of A and B are given in Appendix B.

The stator resistance variation due to temperature or frequency is slowly, in turn, the stator resistance is assumed to be constant during the estimated period. In order to perform computer simulations and implement the Kalman filter algorithm, continuous state equations must be transformed into discrete state equations as follows [11]:

$$x(k+1) = F(k)x(k) + G(k)u(k) \tag{37}$$

$$y(k) = H(k)x(k) \tag{38}$$

where $F(k) = I + A \cdot Ts$, $G(k) = B \cdot Ts$, and $H(k) = C$.

Because of measurement errors and accuracy of the machine model, stochastic variables are introduced, i.e. measurement noise vector $v(k)$ and system noise vector $w(k)$. The discrete-time model can finally be described as:

$$x(k+1) = f(x(k), u(k)) + w(k) \tag{39}$$

$$z(k) = h(x(k)) + v(k) \tag{40}$$

The extended Kalman filter is an optimal estimator in the least-square sense for estimating the states of dynamic nonlinear systems. It involves the linearization approximation of the nonlinear model as follows:

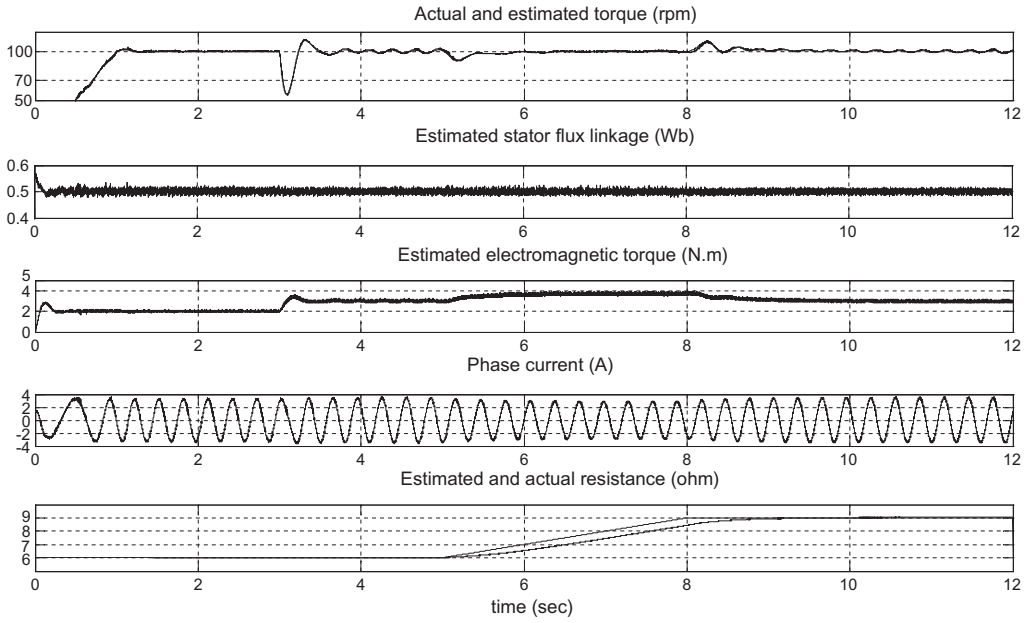

Fig. 3. Simulation waveforms of the sensorless torque/flux SMC scheme (low speed operation).

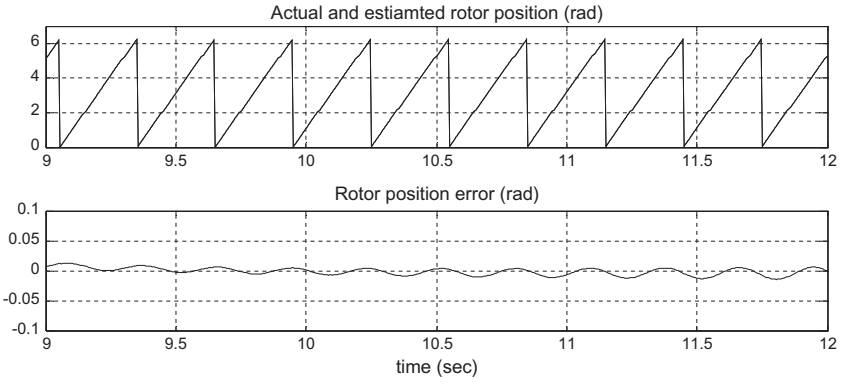

Fig. 4. Actual and estimated rotor position waveforms and the position angle error (low speed operation).

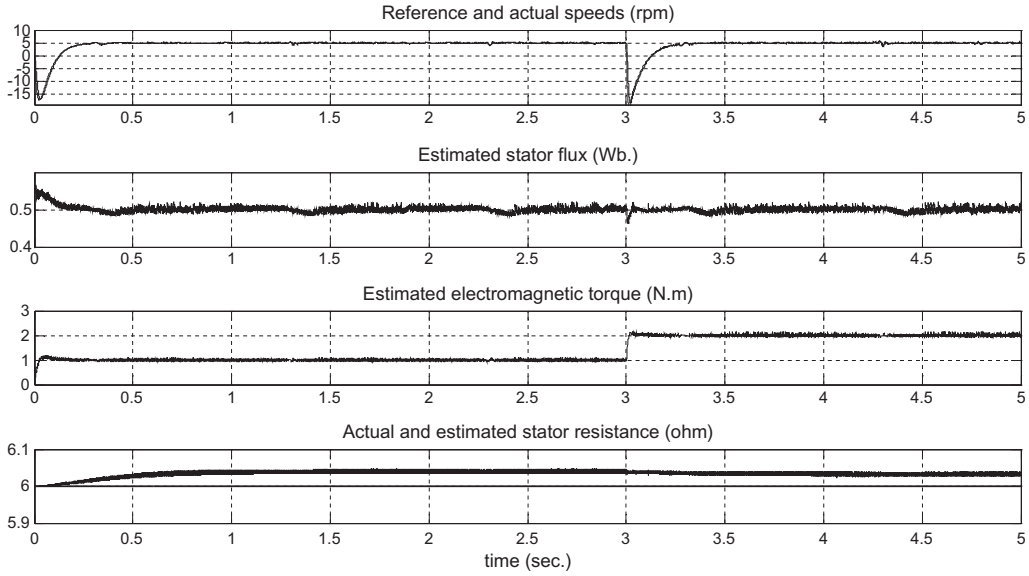

Fig. 5. Simulation waveforms of the sensorless torque/flux SMC scheme (very low speed operation).

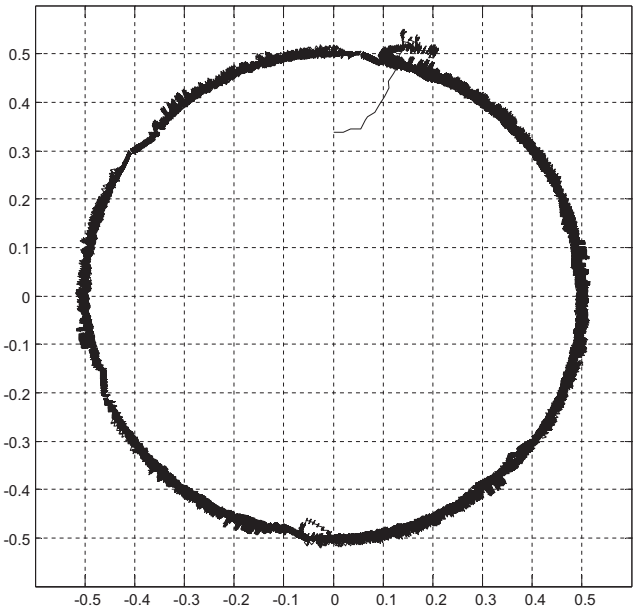

Fig. 6. Locus of the stator flux of the torque/flux SMC in the stationary frame (very low speed).

$$\Gamma(k) = \frac{\partial f(x(k), u(k))}{\partial x(k)}|_{x(k)=\hat{x}(k)} \tag{41}$$

$$\Delta(k) = \frac{\partial h(x(k))}{\partial x(k)}|_{x(k)=\hat{x}(k)} \tag{42}$$

The steps of the EKF algorithm are summarized as [11]:

1- Estimation of the error covariance matrix:

$$P(k+1) = \Gamma(k)P(k)\Gamma^T(k) + Q \tag{43}$$

2- Computation of a Kalman filter gain:

$$K(k) = P(k+1)\cdot\Delta^T(K)\cdot[\Delta(k)\cdot P(k+1)\cdot\Delta(k) + R]^{-1} \tag{44}$$

3- Updating of an error covariance matrix:

$$P(k) = [I - K(k)\cdot\Delta(k)]\cdot P(k+1) \tag{45}$$

4- State estimation:

$$\hat{x}(k+1) = \hat{x}(k) + K(k)[z(k+1) - h(\hat{x}(k+1))] \tag{46}$$

where Q is the covariance matrix of the system noise, namely model error, and R is the covariance matrix of the output noise, namely measurement noise.

To start the calculation, it is necessary to define the initial values of the state variables and the estimation error covariance matrices. The initial values for the matrices Q, R, and P_0 are chosen with a trial–error procedure to get the best tradeoff between filter stability and convergence time.

6. Simulation results

Simulation works are carried out on the IPMSM to prove the effectiveness of the proposed scheme. The simulations are performed using the MATLAB/Simulink simulation package.

Gains of the PI speed controller are selected as: $k_{sp} = 0.007$, $k_{si} = 0.2$.

The reference stator flux is 0.5 Wb. The switching frequency of SVM = 6 kHz.

Sampling time of speed estimator = 10 kHz.

The parameters of the torque/flux sliding mode controller are selected as:

$$K_T = K_\phi = \quad 100,\ K_{cw} = 100,\ \rho = 200,\ K_p = 2,\ K_i = 30.$$

The matrices of the reduced order EKF are selected to be as follows:

$$\mathrm{R} = [0.005\ \ 0;\ 0\ \ 0.005],\ \ \mathrm{P} = [1\ \ 1\ \ 1]\ \text{ and }\ \mathrm{Q} = [100\ \ 100\ \ 0.3]$$

The parameters of the IPMSM are listed in Table 1.

To evaluate the proposed scheme performance, a wide speed range operation with parameters variation and load disturbance are studied in the following sections.

6.1. Case (1) Low speed operation with load disturbance and parameters variation

The reference speed is assumed to be increased from zero to 100 rpm in 1 s. The moment of inertia and damping coefficient are assumed to be increased by 100% at $t = 1$ s. The load torque is

increased steeply from 2 to 3 N m at $t = 3$ s. The stator resistance is increased from 6 Ω (100%) to 9 Ω (150%) in 3 s. The results of the proposed scheme are shown under the specified conditions in Fig. 3. The figure shows that the actual and estimated speeds are aligned and can track well the trajectory of the reference speed. A small dip appears in the estimated and actual speeds at the instant of load disturbance at $t = 3$ s. Compared to the classical DTC [33], the stator flux, electromagnetic torque and phase current waveforms of the proposed scheme contain very low ripples. The estimated stator flux is constant and equals its reference value. The figure shows also that the estimated resistance can trace well the actual resistance. An error between the estimated and actual resistances appears during the variation period, in turn the estimated electromagnetic torque affected. In practical, the stator resistance will take a longer time to change by 50%, in turn; the resistance estimation error will be very small. Fig. 4 shows that the actual and estimated rotor position angles are identical. The results ensure the high performance of the proposed scheme during low speed operation.

6.2. Case (2) Very low speed operation with load disturbance and parameters variation

It is known that the classical DTC performance is unsatisfactory at very low speed operation [29]. To show the effectiveness of the proposed torque/flux SMC scheme, its performance is tested at very low speed operation. In this case, the motor is assumed to be operated at 5 rpm (0.33% of rated speed). The moment of inertia and damping coefficient are assumed to be decreased by 50% at $t = 1$ s. The load torque is increased steeply from 1 to 2 N m at $t = 3$ s. Fig. 5 shows the scheme performance under the previous conditions. It is shown that the actual and estimated speeds are identical. Small dips appear in the actual and estimated speeds at the starting and load disturbance instants. Also, the figure shows that the stator flux and electromagnetic torque waveforms contain low ripples even at very low speed. In addition, the error between the estimated and actual stator resistance is very low (0.05 Ω). Fig. 6 shows the locus of the stator flux in the stationary frame. The stator flux has fast transient response and its components are sinusoidal and displaced in phase by 90°.

6.3. Case (3) High speed operation with load disturbance and parameters variation

In this case, the performance of the proposed scheme is evaluated under high speed operation. The reference speed is increased from zero to 1200 rpm in one second and remains fixed at this value. The load torque is assumed to be increased steeply from 2 to 3 N m at $t = 3$ s. The stator resistance is increased steeply from 6 Ω (100%) to 9 Ω (150%) at $t = 5$ s. The waveforms of the actual

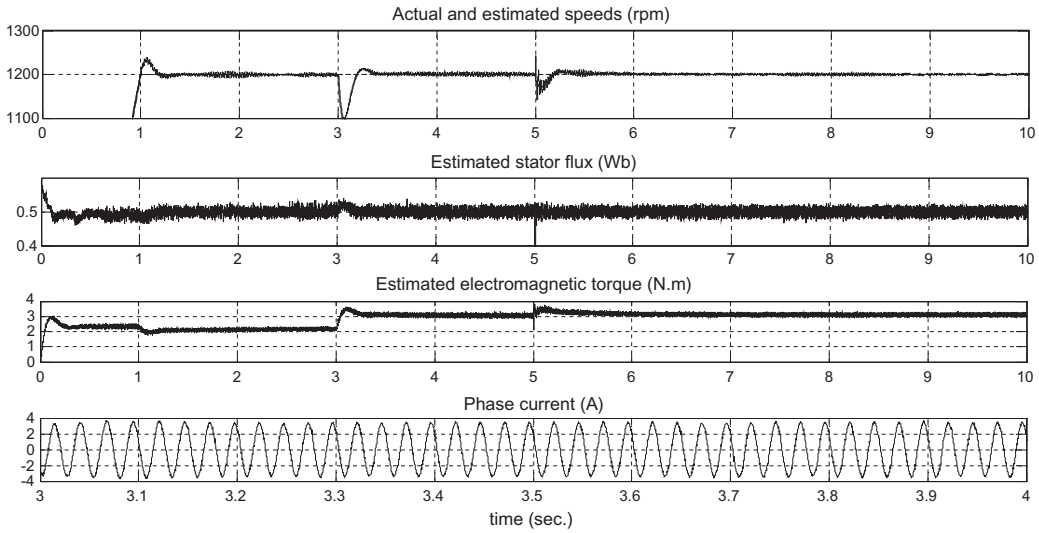

Fig. 7. Simulation waveforms of the sensorless torque/flux SMC scheme (high speed operation).

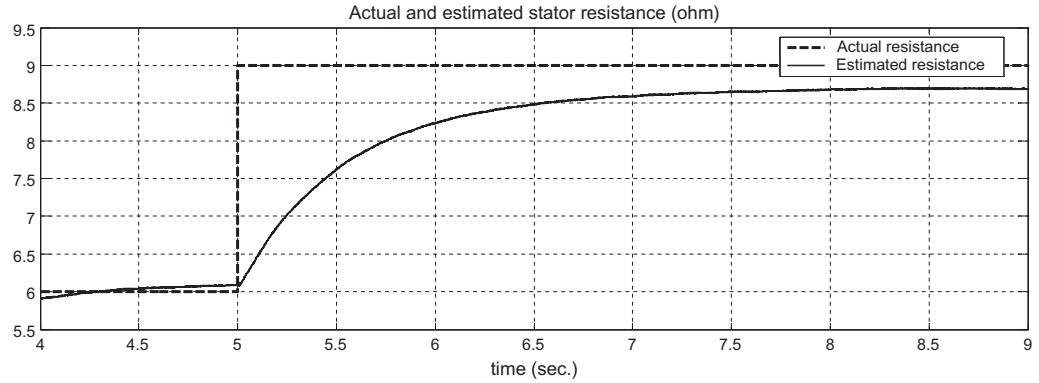

Fig. 8. Actual and estimated stator resistances waveforms (high speed operation).

speed, reference speed, estimated flux, estimated electromagnetic torque and current are shown, respectively, in Fig. 7. The figure shows high frequency oscillations in the estimated speed waveform which can be reduced by introducing a low pass filter and selecting the appropriate cut-off frequency. The flux and the torque ripples percentage at full load are about 4% and 5%, respectively. The phase current waveform is enlarged to show that the motor current is nearly sinusoidal. Fig. 8 shows the variation of the actual and estimated stator resistances. It is shown that the estimated resistance takes about 3 s to reach the actual value and the steady state error about 0.3 Ω (3.33%). The results prove the satisfactory performance of the proposed scheme at high speed operation.

7. Conclusion

Speed sensorless control based on DTC of the IPMSM is studied in this paper. The rotor speed and position angle which required for speed, torque and flux control are estimated based on the active flux concept. To eliminate the problems of the classical DTC, a torque/flux sliding mode controller is designed to replace the hysteresis controllers and the look-up table. To overcome the problem of the stator resistance mismatch, especially at low speed, a reduced order EKF is designed to estimate the stator resistance online. The proposed scheme incorporates the advantages of the DTC, SMC, and sensorless control. Simulation works are carried out to evaluate the proposed scheme performance at different operating conditions. The proposed scheme performance is satisfactory at very low speed as well as high speed operation. The estimated speed can trace well the actual speed, in spite of, load disturbance and parameters variation. The stator flux, torque and current waveforms have low ripples even at very low speed operation. The results prove that the reduced order EKF is able to update the stator resistance online at any operating speed.

Appendix A

Defining Lyapunov function as:

$$V = \frac{1}{2}s^T s \tag{47}$$

The time derivative of V on the state trajectory is given by

$$\dot{V} = s^T \dot{s} \tag{48}$$

Substituting Eq. (16) into Eq. (48), one can obtain:

$$\dot{V} = s^T M + s^T F_n - s^T D_n u + s^T W \tag{49}$$

Substituting the control effort from Eq. (19) into Eq. (49)

$$\dot{V} = s^T M + s^T F_n + s^T W - s^T M - s^T F_n - s^T \alpha_1 \; sign\; (s^T) \tag{40}$$

$$\text{i.e. } \dot{V} = s^T W - \alpha_1 |s^T| \tag{41}$$

for $\alpha_1 > |W|$, Eq. (41) will ensure $\dot{V} \leqslant 0$. This proves the stability of the proposed scheme.

Appendix B

The matrix elements of A and B in Eq. (32)

$$A_{11} = -\frac{R_s}{2L_\pi}(L_\Sigma - L_\Delta \cos 2\hat{\theta}_e) + \frac{\hat{\omega}_e L_\Sigma}{2L_\pi} L_\Delta \sin 2\hat{\theta}_e \tag{42}$$

$$A_{12} = \frac{\hat{\omega}_e L_\Delta}{2L_\pi}(L_\Delta - L_\Sigma \cos 2\hat{\theta}_e) + \frac{R_s}{2L_\pi} L_\Delta \sin 2\hat{\theta}_e \tag{43}$$

$$A_{13} = 0 \tag{44}$$

$$A_{21} = -\frac{\hat{\omega}_e L_\Delta}{2L_\pi}(L_\Delta + L_\Sigma \cos 2\hat{\theta}_e) + \frac{R_s}{2L_\pi} L_\Delta \sin 2\hat{\theta}_e \tag{45}$$

$$A_{22} = -\frac{R_s}{2L_\pi}(L_\Sigma + L_\Delta \cos 2\hat{\theta}_e) - \frac{\hat{\omega}_e L_\Sigma}{2L_\pi} L_\Delta \sin 2\hat{\theta}_e \tag{46}$$

$$A_{23} = 0, \quad A_{31} = 0; \; A_{32} = 0; \; A_{33} = 0 \tag{47}$$

$$B_{11} = \frac{1}{2L_\pi}(L_\Sigma - L_\Delta \cos 2\hat{\theta}_e) \tag{48}$$

$$B_{12} = -\frac{L_\Delta}{2L_\pi} \sin 2\hat{\theta}_e \tag{49}$$

$$B_{13} = \frac{\phi_f}{L_q} \sin \hat{\theta}_e \tag{50}$$

$$B_{21} = -\frac{L_\Delta}{2L_\pi} \sin 2\hat{\theta}_e \tag{51}$$

$$B_{22} = \frac{1}{2L_\pi}(L_\Sigma + L_\Delta \cos 2\hat{\theta}_e) \tag{52}$$

$$B_{23} = -\frac{\phi_f}{L_q} \cos \hat{\theta}_e \tag{53}$$

$$B_{31} = 0; \quad B_{32} = 0; \; B_{33} = 0 \tag{54}$$

where $L_\Sigma = L_d + L_q$, $L_\Delta = L_d - L_q$, $L_\pi = L_q L_d$

References

[1] Morimotor Shigeo, Kawamoto Keisuke, Sanada Masayuki, Takeda Yoji. Sensorless control strategy for salient pole PMSM based on extended EMF in rotating frame. IEEE Trans Indust Appl 2002;38(4):1054–61.

[2] Chen Zhiqian, Tomita Muyuwo, Doki Shinji, Okuma Shigeru. An extended electromotive force model for sensorless control of interior permanent magnet synchronous motors. IEEE Trans Indust Electron 2003;50(2):288–95.

[3] Ichikawa Shinji, Tomita Muyuwo, Doki Shinji, Okuma Shigeru. Sensorless control of permanent magnet synchronous motors using online parameters identification based on system identification theory. IEEE Trans Indust Electron 2006;53(2):363–72.

[4] Corley Matthew J, Lorenz Robert D. Rotor position and velocity estimation for a salient pole permanent magnet synchronous machine at standstill and high speeds. IEEE Trans Indust Appl 1998;34(4):784–9.

[5] Ogasawara Satoshi, Akagi Hirofumi. Implementation and position control performance of a position sensorless IPM motor drive system based on magnetic saliency. IEEE Trans Indust Appl 1998;34(4):806–12.

[6] Choi Chan-Hee, Seok Jul-Ki. Pulsating signal injection based axis switching sensorless control of surface mounted permanent magnet motors for minimal zero current clamping effects. IEEE Trans Indust Appl 2008;44(6):1741–8.

[7] Morimotor Shigeo, Sanada Masayuki, Takeda Yoji. Mechincal sensorless drives of IPMSM with online parameter identification. IEEE Trans Indust Appl 2006;42(5):1241–8.

[8] Hasegawa Masaru, Matsui Keiju. IPMSM position sensorless drives using robust adaptive observer on stationary reference frame. IEEJ Trans 2008;3:120–7.

[9] Hasegawa Masaru, Yoshioka Satoshi, Matsui Keiju. Position sensorless control of interior permanent magnet synchronous motors using unknown input observer for high speed drives. IEEE Trans Indust Appl 2009;45(3):938–46.

[10] Boussak Mohamed. Implementation and experimental investigation of sensorless speed control with initial rotor position estimation for interior permanent magnet synchronous motor drive. IEEE Trans Indust Electron 2005;20(6):1413–22.

[11] Terzic Bozo, Jadric Martin. Design and implementation of the extended Kalman filter for the speed and rotor position estimation of brushless DC motor. IEEE Trans Indust Electron 2001;48(6):1065–73.

[12] Chen Zhiqian, Tomita Muyuwo, Doki Shinji, Okuma Shigeru. New adaptive sliding mode observers for position- and velocity-sensorless controls of brushless motors. IEEE Trans Indust Electron 2000;47(3):582–91.

[13] Rodic Miran, Jezernik Karel. Speed-sensorless sliding mode torque control of an induction motor. IEEE Trans Indust Electron 2002;49(1):87–95.

[14] Lascu Cristian, Boldea Ion, Blaabjerg Frede. Direct torque control of sensorless induction motor drives: a sliding-mode approach. IEEE Trans Indust Appl 2004;40(2):532–90.

[15] Lee Kyo-Beum, Blaabjerg Frede. Sensorless DTC-SVM for induction motor driven by a matrix converter using a parameter estimation strategy. IEEE Trans Indust Electron 2008;55(2):512–21.

[16] Xu Zhuang, Rahman MA. An adaptive sliding stator flux observer for a direct-torque-controlled IPM synchronous motor drive. IEEE Trans Indust Electron 2007;54(5):2398–406.

[17] Liu Yong, Zhu Zi Qiang, Howe David. Instantaneous torque estimation in sensorless direct-torque-controlled brushless DC motors. IEEE Trans Indust Appl 2006;42(5):1275–83.

[18] Andreescu Gheorghe-Daniel, Pitic Cristian Ilie, Blaabjerg Frede, Boldea Ion. Combined flux observer with signal injection enhancement for wide speed range sensorless direct torque control of IPMSM drives. IEEE Trans Energy Convers 2008;23(2):393–402.

[19] Foo G, Rahman MF. Sensorless sliding-mode MTPA control of an IPM synchronous motor drive using a sliding mode observer and HF signal injection. IEEE Trans Indust Electron 2010;57(4):395–403.
[20] Rahman Muhammed Fazlur, Zhong L, Enamul Haque Md, Rahman MA. A direct torque-controlled interior permanent magnet synchronous motor drive without a speed sensor. IEEE Trans Energy Convers 2003;18(1):17–22.
[21] Boldea Ion, Paicu Mihaela Codruta, Andreescu Gheorghe-Daniel, Blaabjerg Frede. Active flux" DTFC-SVM sensorless control of IPMSM. IEEE Trans Energy Convers 2009;24(2):314–22.
[22] Foo G, Rahman MF. Sensorless direct torque and flux controlled IPM synchronous motor drive at very low speed without signal injection. IEEE Trans Indust Electron 2010;57(1):395–403.
[23] Haque ME, Rahman MF. Influence of the stator resistance variation on direct torque controlled interior permanent magnet synchronous motor drive performance and compensation. In: Thirty-sixth IAS annual meeting conference record of the 2001. IEEE. p. 2563–9.
[24] Han Yoon-Seok, Choi Jung-Soo, Kim Young-seok. Sensorless PMSM drive with a sliding mode control based adaptive speed and stator resistance estimator. IEEE Trans Magnet 2000;36(5):3588–91.
[25] Lee Kyu-Wang, Jung Doo-Hee, Ha In-Joong. An online identification method for both stator resistance and back-emf coefficient of PMSMs without rotational transducers. IEEE Trans Indust Electron 2004;51(2):507–10.
[26] Zhong L, Rahman MF, Hu WY, Lim KW, Rahman MA. A direct torque controller for permanent magnet synchronous motor drives. IEEE Trans Energy Convers 1999;14(3):637–42.
[27] Zhong L, Rahman MF, Lim KW, Zhong L. A direct torque controlled interior permanent magnet synchronous motor drive incorporating field weakening. IEEE Trans Indust Appl 1998;34(6):1246–53.
[28] Wang Yu, Deng Zhiquan. An integration algorithm for stator flux estimation of a direct-torque-controlled electrical excitation flux-switching generator. IEEE Trans Energy Convers 2012;27(2):411–20.
[29] Tang Lixin, Rahman MF, Zhong L, Enamul Haque Md. Problems associated with the direct torque control permanent magnet synchronous motor drive and their remedies. IEEE Trans Indust Electron 2004;51(4):799–809.
[30] Buja Giuseppe S, Kazmierkowski Marian P. Direct torque control of PWM inverter fed ac machine – a survey. IEEE Trans Indust Electron 2004;51(4): 744–57.
[31] Nasir Uddin M, Hafeez Muhammad. FLC-based DTC scheme to improve the dynamic performance of an IM drive. IEEE Trans Indust Appl 2012;48(2): 823–31.
[32] Jidin Auzani, Idris Nik Rumzi Nik, Yatim Abdul Halim Mohamed, Sutikno Tole, Elbuluk Malik E. Simple dynamic overmodulation strategy for fast torque control in DTC of induction machines with constant switching-frequency controller. IEEE Trans Indust Appl 2011;47(5):2283–91.
[33] Fnag CH, Huang CH, Lin SK. Adaptive sliding mode torque control of PM synchronous motor. IEE Proc Power Appl 2001;149(3):228–36.
[34] Wai Rong Jong. Adaptive sliding mode control for induction servomotor drive. IEE Proc Power Appl 2000;147(6):553–62.
[35] Hassan AA, Mohamed YS, Shehata EG. Cascade sliding mode torque control of a permanent magnet synchronous motor. IEEE Int Conf Indust Technol, ICIT 2006:465–70.
[36] Carmeli MS, Mauri M. Direct torque control as variable structure control: existence conditions verification and analysis. Electric Power Syst. Res. 2011;81:1188–96.